Astrophysical light scattering problems (PAP316)

Lecture 6a & 6b

Karri Muinonen
Academy Professor
Department of Physics, University of Helsinki, Finland

Interplanetary dust, Contents

- Introduction, Interplanetary dust particles (IDPs)
- Polarimetric observations of the zodiacal light
  - Historical background
  - Zodiacal light intensity and polarization
  - Solar F-corona observations
  - Circular polarization observations
- Local values of the zodiacal polarization
  - The inversion method
  - Radial variation of the local polarization
  - Polarization-phase curve
- Analysis of the observations and interpretations
  - Properties of the interplanetary particles
  - Numerical simulations of the polarization of the zodiacal light
  - Possible origin of circular polarization
- Discussion
  - Thermal equilibrium of the dust population
  - Experimental simulations
  - Dust particle physical properties and their sources
  - Perspectives

Introduction (1/2)

- Physical characterization of astronomical objects (e.g., surfaces of airless planetary objects)
- Direct problem of light scattering by particles with varying particle size, shape, refractive index, and spatial distribution
- Inverse problem based on astronomical observations and/or experimental measurements
- Plane of scattering, scattering angle, solar phase angle, degree of linear polarization

Introduction (2/2)

- Interplanetary dust
  - optically thin, lenticular dust cloud
  - at 1 au, a few particles within a cubic kilometer
  - zodiacal light
  - gegenschein
- Polarimetry
  - positive and negative polarization
  - complementary inverse problems of interplanetary, cometary, and asteroidal dust

FIGURE 24.1 Zodiacal light seen from Paranal, Chile, 06/2008. Jupiter can be seen at the top of the image.

Credit: ESO/Y. Beletsky

Polarimetric observations of the zodiacal light

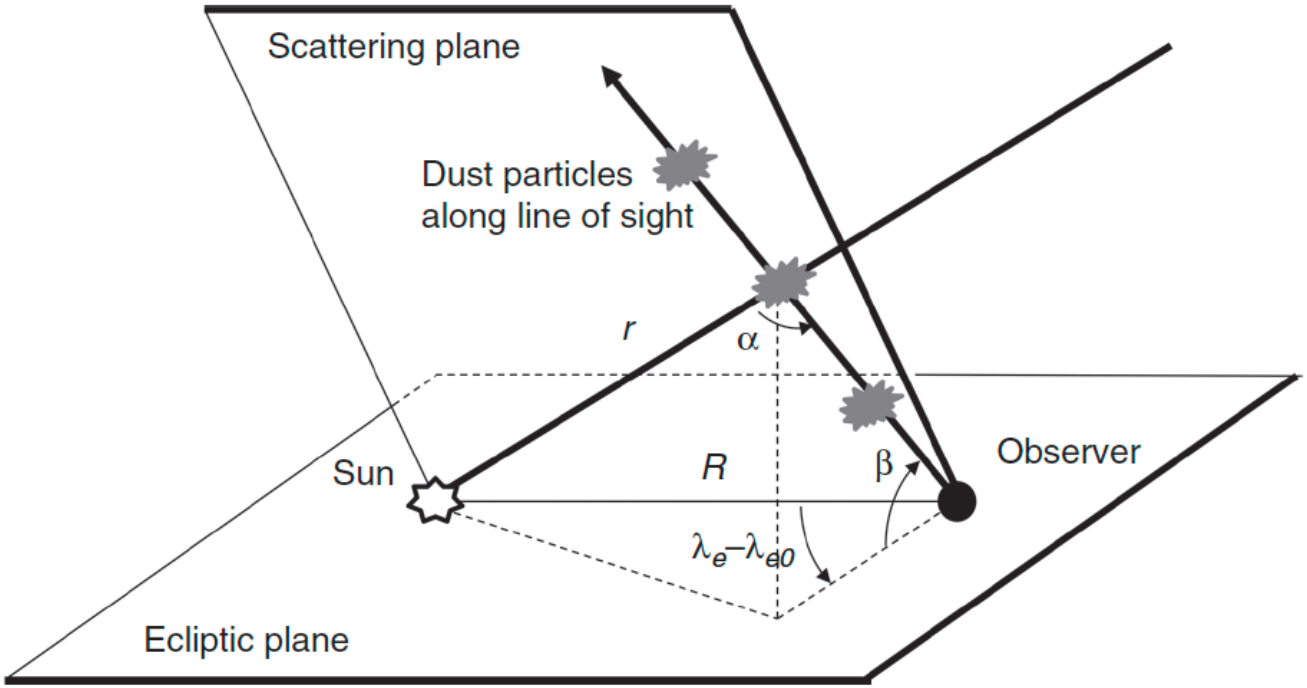

FIGURE 24.2 Geometry of observation of the zodiacal light with representation of the characteristics used in the text.

Adapted from Levasseur-Regourd *et al.* (2007).

- Zodiacal light studied by Cassini (1690)
- Gegenschein reported by Brorsen (1854)
- Ecliptic latitude and helio-ecliptic longitude

Zodiacal light intensity and polarization

- Entanglement with atmospheric, galactic, and extragalactic glows
- Annual variations due to the Earth's orbital motion
- Symmetry plane tilted from the ecliptic, possibly warped
- Degree of polarization shows S-type asteroid wavelength dependence

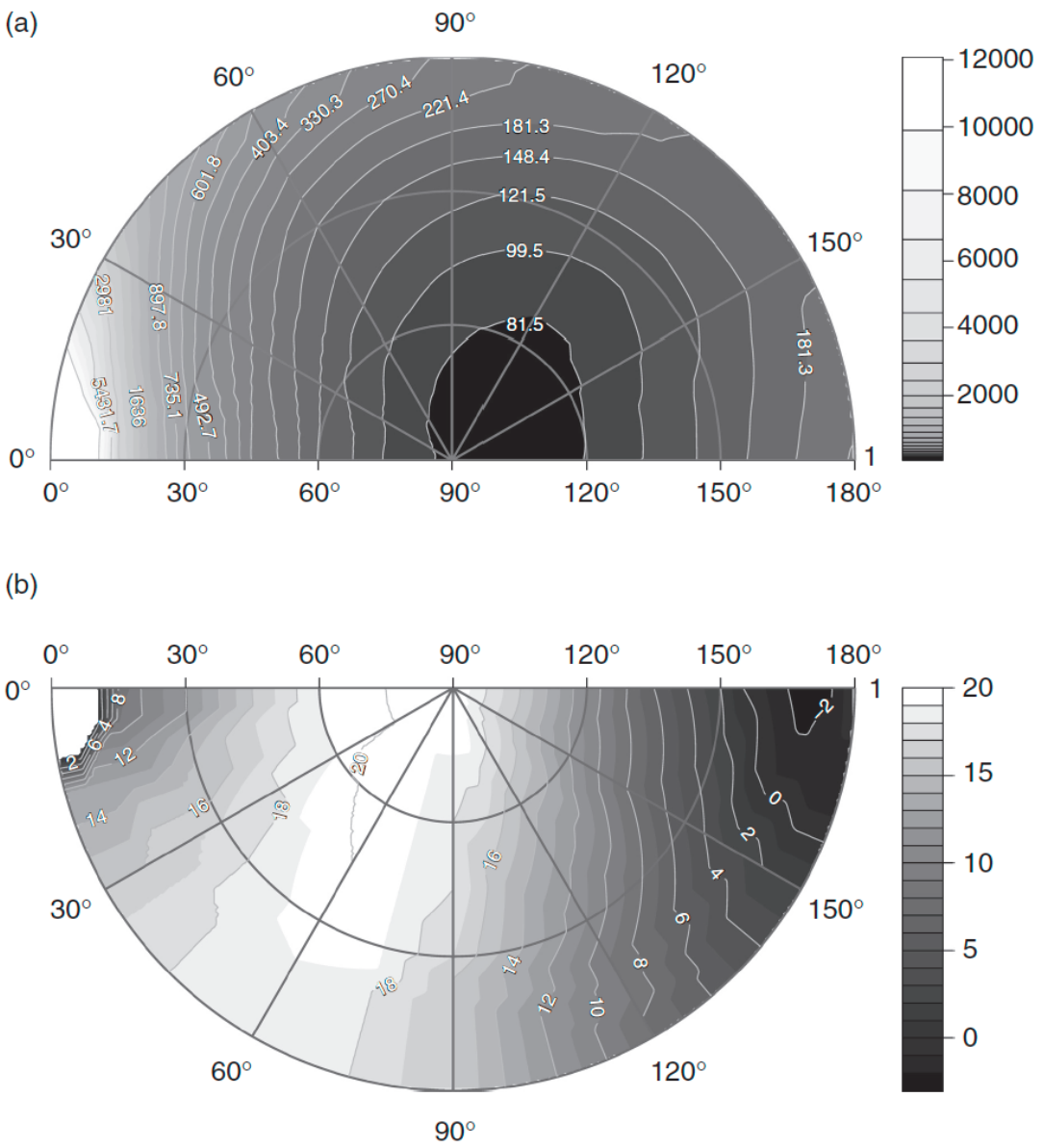

FIGURE 24.3 Above: map of the zodiacal light intensity (10^{-8} W m^{-2} sr^{-1} μm^{-1}) at 550 nm. Below: map of the zodiacal polarization. The outer circle represents the ecliptic, the point at 0° is the Sun and the central point is the ecliptic pole. Values are corrected for oscillations induced by the slight inclination of the zodiacal light symmetry plane and the Earth's orbit eccentricity.

Based on the data from Dumont and Sanchez (1975a) and Leinert *et al.* (1998).

TABLE 24.1. Zodiacal light polarization P_Q (in %), measured from the Earth in the visible domain, typically near 550 nm[1]

β	0°	5°	10°	15°	20°	25°	30°	45°	60°	75°	90°
$\lambda_e - \lambda_{eo}$											
0°				8	10	11	12	16	19	20	20
5°				9	10	11	12	16	19	20	20
10°			11	1 1	12	13	14	17	19	20	20
15°	13	13	13	13	13	14	15	17	19	20	20
20°	14	14	14	15	15	15	15	17	19	20	20
25°	15	15	15	16	16	16	16	18	19	20	20
30°	16	16	16	16	16	17	17	18	19	20	20
35°	17	17	17	17	17	17	17	18	20	20	20
40°	17	17	17	17	18	18	18	19	20	20	20
45°	18	18	18	18	18	18	18	19	20	20	20
60°	19	19	19	19	19	20	20	20	20	20	20
75°	18	18	18	18	18	19	19	19	19	19	20
90°	16	16	16	16	16	16	17	18	18	19	20
105°	12	12	12	12	13	13	14	15	17	19	20
120°	8	8	9	9	9	10	11	13	15	18	20
135°	5	5	5	6	6	7	8	11	14	17	20
150°	2	2	2	3	3	4	5	8	12	16	20
165°	–2	–2	–1	–1	0	2	3	7	11	16	20
180°	0	–2	–3	–2	–1	0	2	6	11	16	20

[1] The directions are defined by their ecliptic latitude (β) and helio-ecliptic longitude ($\lambda_e - \lambda_{eo}$), once the corrections for the slight inclination of the symmetry plane and for the Earth's orbit eccentricity have been made (Levasseur-Regourd *et al*. 2001).

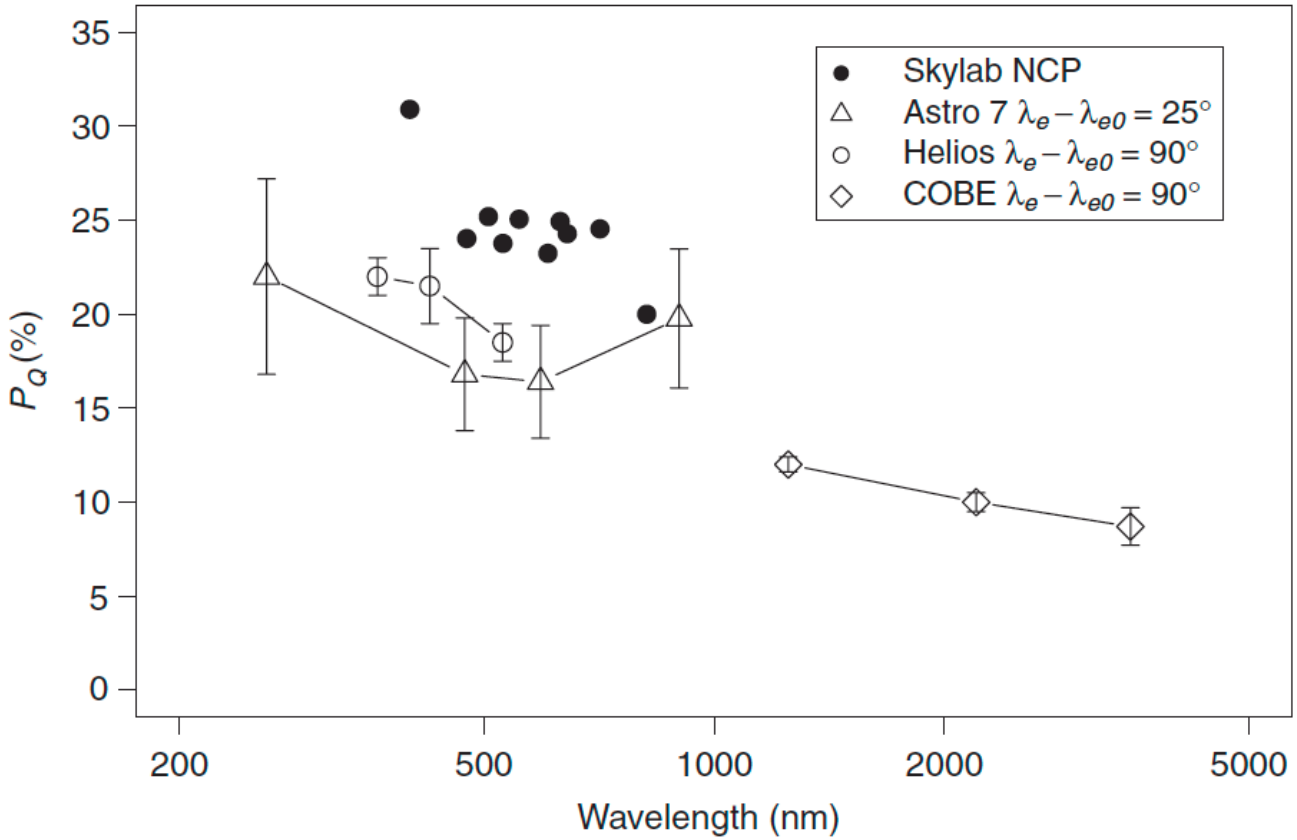

FIGURE 24.4 Wavelength variation of P_Q in different directions in the sky. • Skylab at the north celestial pole (Weinberg and Hahn 1980); △ rocket Astro 7 (Pitz *et al.* 1979); ○ Helios (Leinert *et al.* 1982); ◇ COBE (Berriman *et al.* 1994).

Solar F-corona observations

- Beyond 4 solar radii from the Sun's surface, F-corona shows polarization presumed to be related to light scattering by dust
- Polarization not consistent with the mechanism of light scattering
- F-corona polarization remains to be modeled from first principles of physics

Circular polarization observations

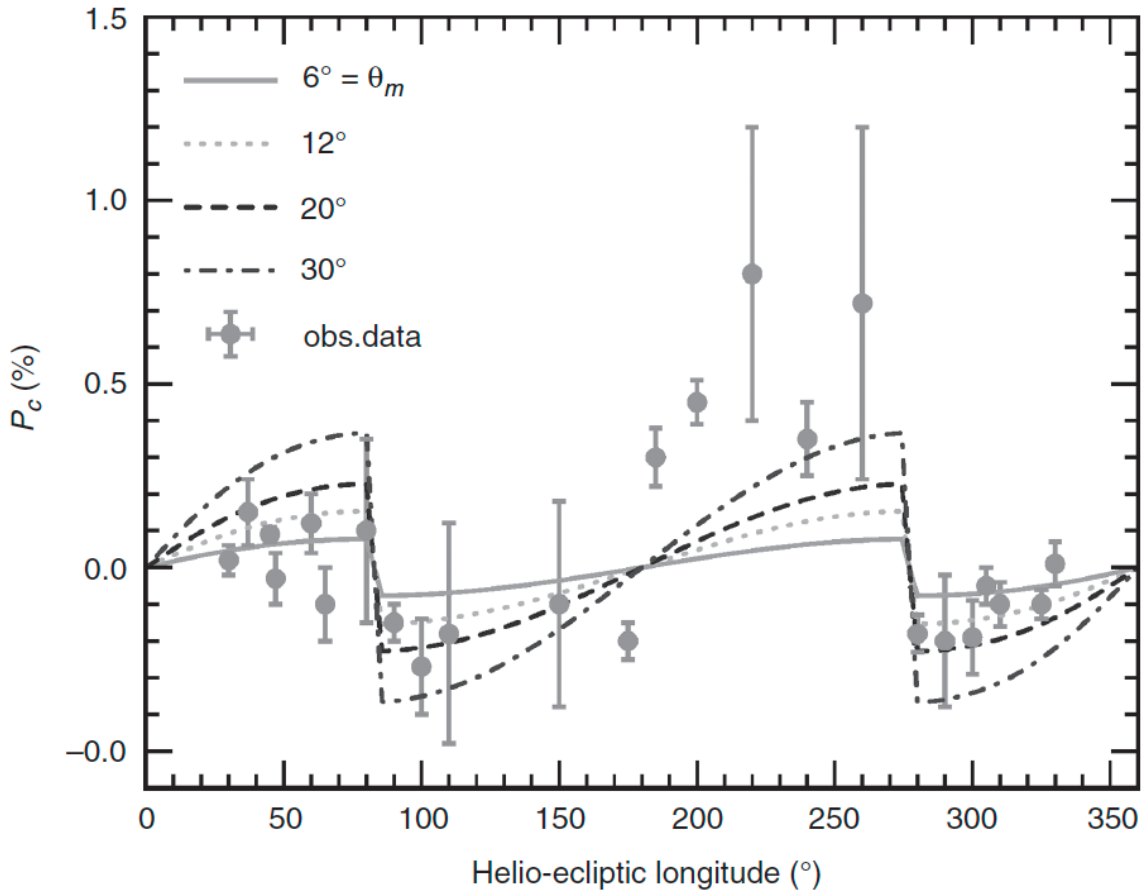

FIGURE 24.5 Circular polarization, P_c, as a function of the helio-ecliptic longitude ($\lambda_e - \lambda_{eo}$), for different angles, θ_m, between the solar magnetic field and the ecliptic plane. The vertical component of the magnetic field is reversed for ($\lambda_e - \lambda_{eo}$) smaller than 90° and ($\lambda_e - \lambda_{eo}$) larger than 270°. Data from Wolstencroft and Kemp (1972) and Staude and Schmidt (1972), lines show results of the modeling.

Hoang and Lazarian (2014).

- Partial alignment of asymmetrical particles can cause circular polarization
- Varying degrees of circular polarization observed

Local values of the zodiacal polarization

TABLE 24.2 Variation of the dust local properties in the symmetry plane[2]

	Value at 1 au	Gradient (exponent in the power law)	Domain (au)
Intensity	about 23×10^{-7}	-1.25 ± 0.02	0.5 to 1.4
Linear polarization	0.3 ± 0.03	$+0.5 \pm 0.1$	0.5 to 1.4
Temperature	$250\ \mathrm{K} \pm 10\ \mathrm{K}$	-0.36 ± 0.03	1.1 to 1.4
Albedo	0.07 ± 0.03	-0.34 ± 0.05	1.1 to 1.4
Space density	$10^{-19}\ \mathrm{kg.m^{-3}}$	-0.93 ± 0.07	1.1 to 1.4

[2] The variations in the local properties, as a function of the solar distance, r, is described with a power law assumption. The optical properties (linear polarization, albedo, and intensity in W m^{-2} sr^{-1} μm^{-1} rad^{-1} at 550 nm) are retrieved at $\alpha = 90°$ (Levasseur-Regourd 1996; Levasseur-Regourd *et al.* 2001). The density of the particles is inferred from the inverted values of i and p.

- Local intensity and polarization values derived from an inverse problem
- Rigorous inversion possible in the direction of observer motion (optical probe technique)
- General problem treated, e.g., by Lumme (2000)

Radial variation of local polarization

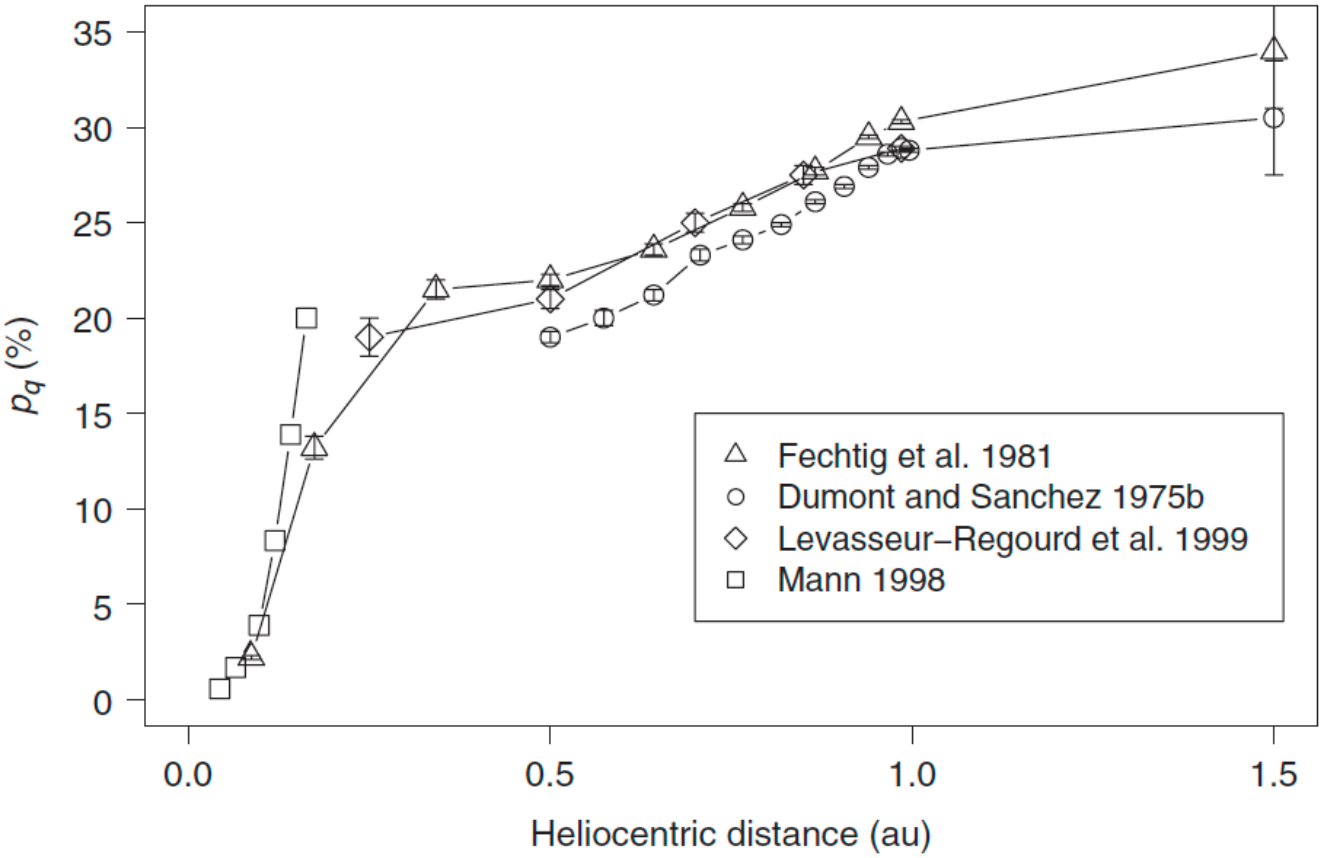

FIGURE 24.6 Variation of the local linear polarization, p_q, at $\alpha = 90°$ as a function of the heliocentric distance (au)

Data adapted from Fechtig *et al.* (1981), Dumont and Sanchez (1975b), Levasseur-Regourd *et al.* (1991), Mann (1998), and Levasseur-Regourd *et al.* (1999).

- Scattering properties of dust not constant within the cloud
- Temporal variation due to dust particle spiraling to the Sun (Poynting-Robertson effect)
- ~r^{1} gradient in local density, different from that for homogeneous dust ($r^{1.3}$)

Polarization-phase curve

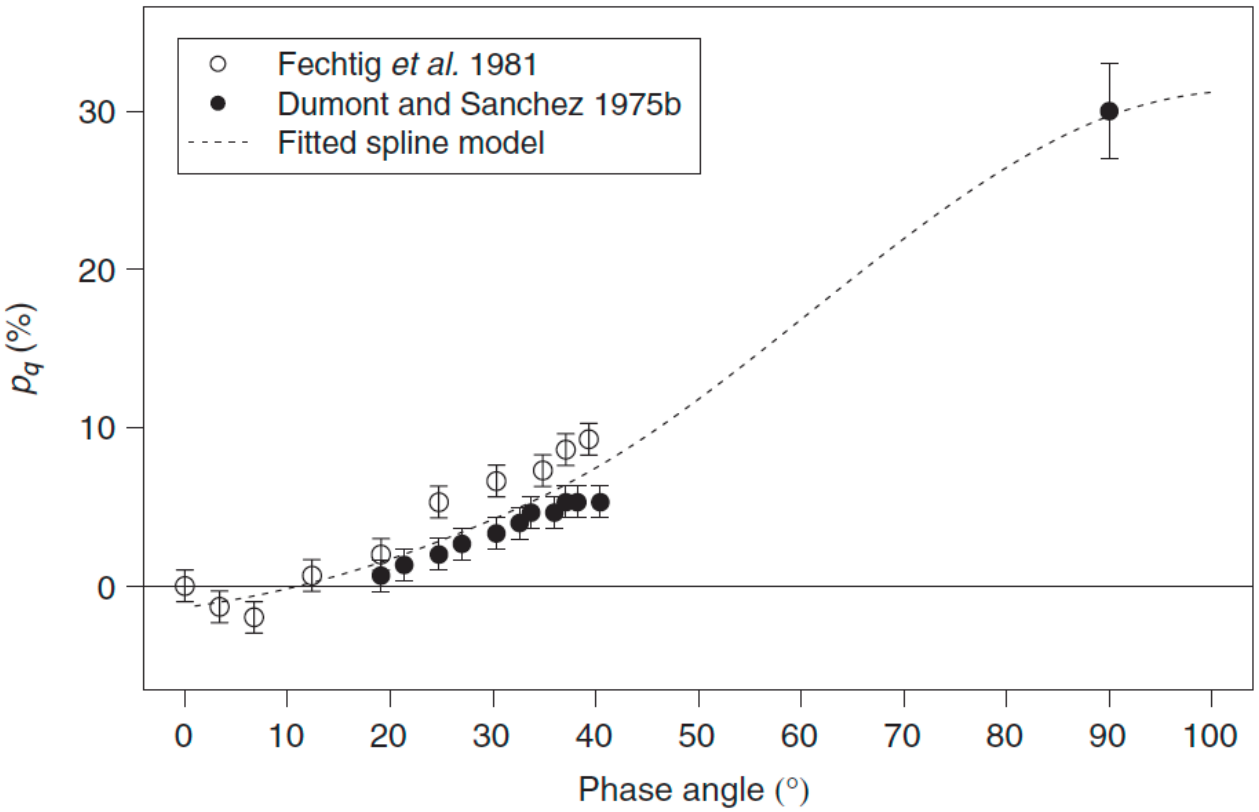

FIGURE 24.7 Variation of the local linear polarization, p_q, as a function of the phase angle at 1.5 au.

Data inverted from Fechtig *et al.* (1981), Levasseur-Regourd (1996), and Renard *et al.* (1995).

- Polarimetric phase curve comparable to that of cometary dust or of C-type asteroids
- Scattering by irregular dust particles and/or fluffy aggregates of submicron (absorbing) grains

Properties of the interplanetary dust particles

- Cometary dust
  - fluffy, easily fragmenting
- Asteroidal dust
  - compact particles from asteroid shattering
- Interstellar dust
  - submicron grains passing through
  - a priori not linked to primordial grains forming the Solar System
- Particle size distribution
  - power law index -3 for sizes <20 microns
  - -4.4 for sizes >20 microns
  - typical sizes 5-25 microns
- Silicates and organic materials
  - Mg-rich pyroxenes
  - amorphous carbon and organic carbon
  - polycyclic aromatic hydrocarbon molecules (PAH)

Numerical simulations of the polarization of the zodiacal light

- Early studies using Mie theory for spherical particles
- Spheroids and aggregates of spheroids
- Irregular particles

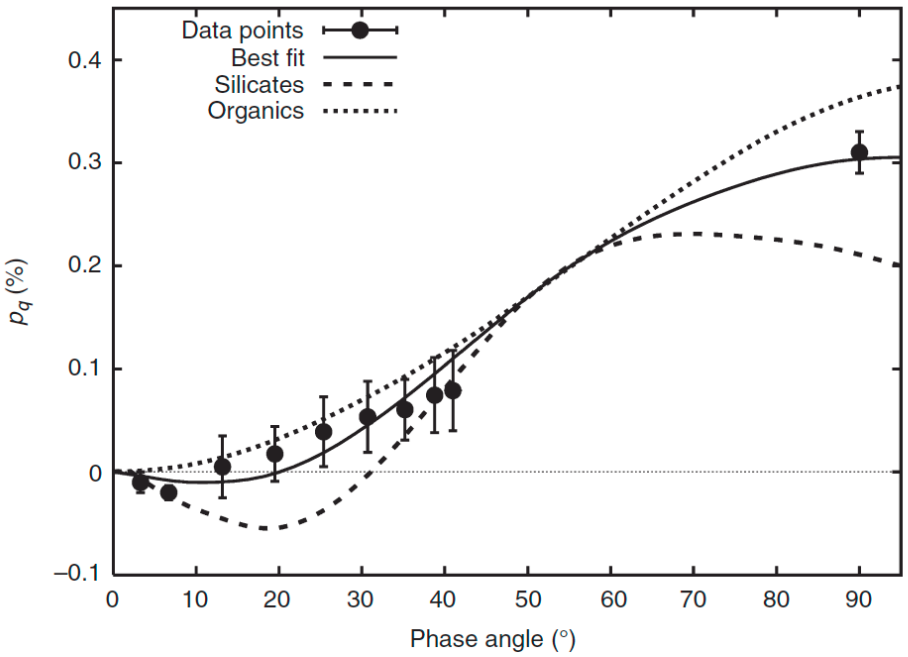

FIGURE 24.8 Comparison between the phase function of the local linear polarization, p_q, at 1.5 au and the numerical model of light scattering by IDPs with aggregates of silicates, organics, and a mixture of both compositions.

Reproduced from Lasue *et al.* (2007) with permission © ESO.

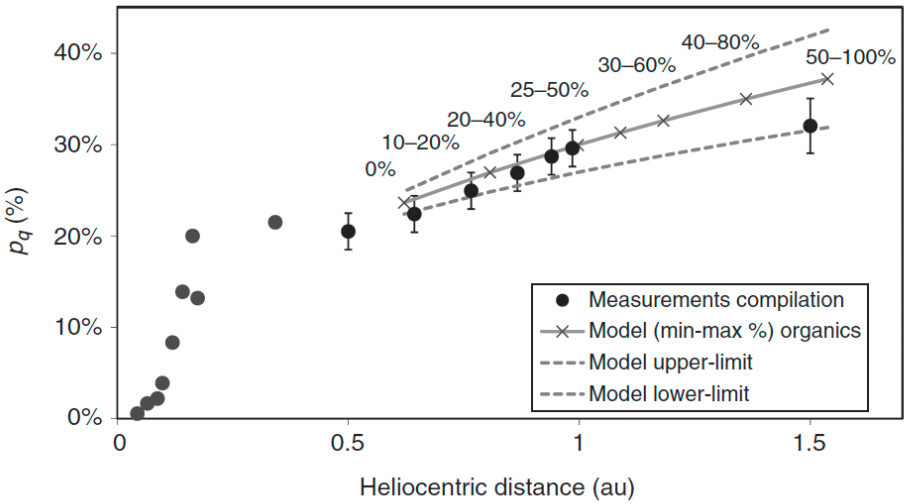

FIGURE 24.9 Comparison between the local linear polarization, p_q, as a function of the heliocentric distance (au) at $\alpha = 90°$ and the numerical model of polarization from a cloud of IDPs constituted of aggregates with varying silicates to organics ratio (labeled on the graph). The lower and upper limits shown represent the uncertainties in the continuous functions models from Table 24.2.

Reproduced from Lasue *et al.* (2007) with permission © ESO.

Possible origin of circular polarization

- Aligned nonspherical particles
- Influence of both solar wind and magnetic fields
- Radiative torque alignment plays a major role (cf. Herranen, Ph.D. thesis, 2020), coupling with the magnetic fields
- Circular polarization may offer a tool to study the interplanetary magnetic fields

Discussion

Thermal equilibrium of the dust population

- Significant population of absorbing particles consistent with the temperature variations of the particles
- Absolute temperature more agreeable with low-absorbing and compact particles (!)

Experimental simulations

- Similar degrees of polarization measured for large dark and irregular particles and mixtures of large fluffy aggregates of silica and carbon materials

Dust particle physical properties and their sources

- Two major sources
  - main asteroid belt (~50%)
  - comets (~50%)
- Minor contributions
  - Kuiper Belt
  - interstellar medium
- In agreement with IDPs collected in the Earth's stratosphere
- Tentative agreement with polarimetric imaging of
  - exozodiacal dust with silicates and ice-filled fluffy aggregates
  - young debris disks with ongoing dust aggregation
- Obs! Extrasolar systems may differ substantially from our Solar System

Perspectives

- Progress from line-of-sight intensity and polarization to local values
- Physical particle models from polarization consistent with other data
- Particle origin and properties continue to be debated
- Future observations at all wavelengths, potentially out of the ecliptic
- Wide-angle ground-based cameras
- JAXA Akatsuki mission, student Eye-Sat nanosatellite